

Service Guarantees Countering Renewable Generation Uncertainty in Multi-microgrids

Arnab Dey¹, *Student Member, IEEE*, Vivek Khatana¹, *Student Member, IEEE*, Ankur Mani²,
and Murti V. Salapaka¹, *Fellow, IEEE*

Abstract—With increased penetration of Renewable Energy Systems (RES), the conventional distribution grid is advancing towards Interconnected multi-microgrid systems (IMMG) supervised by a Distribution Network Operator (DNO). However, the inherent uncertainty of RES poses a challenge in meeting the power demand of critical infrastructures in the microgrids unless sufficient battery storage is maintained. Yet, maintaining expensive battery storage increases the operating cost. In this article, we propose a dynamic energy resource allocation strategy to optimize the battery reserve requirement while ensuring that critical demand is met with a provable guarantee. Our solution is built upon stochastic control techniques. Under our proposed scheme, the DNO responds to the evolving uncertainty by dynamically balancing the RES and battery resources and eliminates the risk of over or underproduction. We derive battery reserve allocation strategy for multi-microgrid systems in *two* settings: when microgrids *can* (interconnected) and *cannot* (individualized) share power amongst each other. We present numerical simulations under different scenarios with detailed comparison of the performance of the proposed algorithm for individualized and shared settings. The simulation results demonstrate the efficacy of our algorithm. In particular, it quantifies value of connecting microgrids through savings in battery requirements under IMMG over individualized microgrids.

Index terms: Multi-microgrid, optimization, partial differential equations, renewable energy sources, resource allocation, stochastic process, uncertainty minimization, wind energy.

I. INTRODUCTION

IN recent times, the proliferation of distributed energy resources (DER), propelled by a mounting interest towards the generation and utilization of clean renewable energies, has fostered a paradigm change in the operation and control of power distribution networks. Renewable energy sources (RES), like solar and wind energy systems, reduce the adverse environmental effects of traditional energy sources; integration of DERs also offer improved grid assistance, efficiency and reliability. As renewables are expected to contribute 60% of total generation by 2050 [1], a rapid growth of ‘prosumers’, equipped with distributed RES, is envisaged to transform the conventional energy systems to an ecosystem of multiple individual microgrids (MGs). Here, due to the intermittent nature of RES, the MGs are exposed to the risk of underproduction

if extra measures such as mechanisms for ancillary services are not present [2]. Similarly, uncertainty of RES, exacerbated by excess provisioning of ancillary services, such as energy storage, can result into overproduction which increases the operating cost. Since both overproduction and underproduction are undesirable, an important question that needs to be answered is: how can the MGs guarantee this demand supply balance? In this context, energy storage allocation for demand-supply balance, considering fluctuating renewable generation, is of significant interest [3]–[7]. However, works which are primarily focused on guaranteeing load demand of multiple critical facilities under generation uncertainty, in a multi-microgrid framework, are still in their nascent stages. In the context of system reliability, various optimization techniques [5]–[9] are used. Analytical approaches to improve power balance in systems with multiple MGs are devised in [10]–[11]. Prior works have also considered game theoretic approaches [12]–[13], stochastic programming [14], and, model-predictive control [15] to improve system resiliency with high penetration of RES, however without explicitly modelling the RES output. A battery charging and discharging policy is proposed in [16], to reduce the power imbalance due to RES uncertainty with explicit stochastic model for RES. However, no provable guarantee of meeting the demand is provided.

The problem of assuring the demand-supply balance is coupled with proper provisioning of battery energy storage. Maintaining excess battery storage increases the investment and operating cost. Therefore, determining the optimal amount of energy storage to be maintained, with uncertain RES, is an important issue [17]–[21]. In an Individualized Multi-microgrid (IDMMG) system, energy sharing among MGs is not allowed which leads to large energy reserve requirement. In this context, collaborative operation across multiple facilities allows for risk pooling between RES and reduce the storage needed to maintain the guarantee of demand-supply balance. This leads to an integrated and flexible framework of Interconnected Multi-microgrids (IMMGs). However, the additional benefits of IMMG over IDMMG must be quantified to justify the utility of IMMG. Various optimization algorithms focusing on cost benefit of multi-microgrid architectures are proposed in [22]–[25]. Note that guarantee of supplying critical loads under unforeseen generation outage is difficult to obtain here as the methodologies depend on RES forecast or historical values. A careful observation reveals that most of the existing works either focus on cost optimization for energy trading in IMMG without addressing the supply guarantee required by the critical infrastructures (e.g. hospitals), or, solely consider energy storage optimization without exploring

This work is supported by Advanced Research Projects Agency-Energy OPEN through the project titled "Rapidly Viable Sustained Grid" via grant no. DE-AR0001016.

¹Arnab Dey (e-mail: dey00011@umn.edu), Vivek Khatana (e-mail: khata010@umn.edu), and Murti V. Salapaka (e-mail: murtis@umn.edu) are with Department of Electrical and Computer Engineering, University of Minnesota, Twin Cities, USA, and ²Ankur Mani (e-mail: amani@umn.edu) is with Department of Industrial and Systems Engineering, University of Minnesota, Twin Cities, USA.

the benefit of cooperation under RES uncertainty. In summary, assurance of meeting the power demand of critical infrastructures in multi-microgrid setting along with quantitative analysis of cooperation benefit is limited in literature.

To this end, in this article we focus on an IMMIG framework consisting of centralized battery storage and multiple small-scale MGs with critical infrastructures that require a *guarantee* of supplying the demand requested at a pre-specified future time. Each MG is equipped with RES which are uncertain in nature, thus posing a risk of not being able to meet the local critical demand. To mitigate this uncertainty, the Distribution network operator (DNO), which supervises the IMMIG, allocates battery storage to support the MGs while managing how they share renewable energy with each other. The focus of the article is on the optimal allocation of battery storage and dynamic re-balancing by the DNO to meet the power demand of each MG at the requested time to create a reliable grid-independent IMMIG system. The major contributions are summarized below:

(i) We study an IMMIG managed by a DNO, which controls the energy sharing among the MGs. We provide a solution to the problem of initial battery storage provisioning with the objective of meeting power demand of each prosumer at a future pre-specified time with provable guarantees, in presence of stochasticity of the RES. Such a guarantee is essential for critical applications under catastrophic events. Here, we establish that the optimal initial provisioning of energy storage decided by our algorithm is such that (i) any smaller provisioning will lead to scenarios where demand cannot be met, (ii) any larger provisioning will lead to scenarios where generation exceeds the demand. We emphasize that with our optimal initial provisioning both cases (i) and (ii) above are avoided almost surely, that is, with probability one. Thus initial battery provisioning per our solution eliminates risks of underproduction and overproduction at the future pre-specified time, when critical demand is requested, with provable guarantee that the demand is met even in the presence of uncertainty in RES.

(ii) We provide exact solutions for continuous time resource allocations for the DNO to manage renewable and battery resources. Our solution builds upon stochastic control techniques. We provide a practical algorithm for discrete time battery resource management. We remark that such a solution is pertinent for supporting critical infrastructures.

(iii) We present a comparative study with a IDMMG based approach where energy sharing among the prosumers is not possible and the DNO is solely responsible to meet the critical load demands of the prosumers by dynamic allocation of renewable and battery storage. The solution is compared to the IMMIG framework to show the advantage of cooperation in IMMIG with high penetration of DER and critical loads.

The rest of the paper is organized as follows: The description of the IMMIG is provided in Section II. A problem formulation is introduced in Section III. Section IV describes the proposed resource allocation algorithms for both IDMMG and IMMIG and the simulation results are shown in Section V. Section VI presents the concluding remarks.

II. SYSTEM DESCRIPTION

Renewable based large distribution networks, with centralized battery storage [26], consist of several small-scale MGs geographically apart from each other, under the supervision of DNO. We consider such an islanded distributed framework constituting an IMMIG, where the DNO can operate the network more efficiently than IDMMG by utilising the ability of cooperation between the MGs. Fig. 1 shows the hierarchical architecture of the IMMIG under consideration, which contains N_m microgrids and a DNO which controls the energy transaction among the microgrids and dispatches the centralized battery units, based on the requirements, to maintain system reliability. Each MG has RES to supply its local demands. However, the uncertain nature of RES poses the risk of either power deficit, when generation is less than demand, or excess power that forces curtailment, when generation exceeds demand. In IDMMG, this risk is minimized by using independent energy storage systems such as batteries for individual MG, thus requiring large ancillary battery energy storage systems (BESS) [27]. In contrast, an IMMIG, as shown in Fig. 1, enables MGs to share energy among each other in a controlled fashion to maintain demand-supply balance, where excess generation from one MG is utilized to minimize the deficit of another, instead of power curtailment, thus reducing the amount of BESS. DNO controls the energy transactions and the dispatch of batteries. A communication layer is used to transmit real-time power measurements of individual MG to aid the DNO for efficient resource allocation. To reduce the energy cost, the DNO needs to estimate optimal battery storage while ensuring that the load demands of the MGs are met, irrespective of the irregularities of RES. In the subsequent sections we formally introduce the problem and provide a solution along with a comparison with IDMMG.

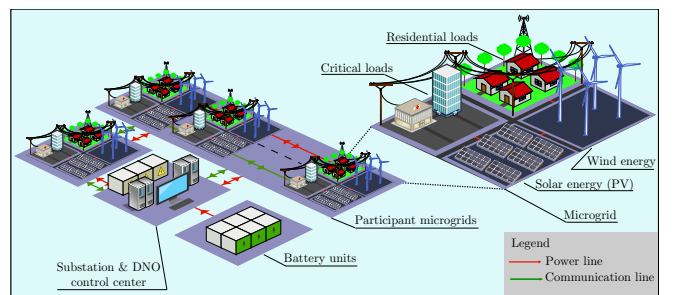


Fig. 1. IMMIG architecture with centralized BESS and microgrids with RES.

III. PROBLEM FORMULATION

Let $\mathcal{I} = \{1, 2, \dots, N_m\}$ denote the set of microgrids present in the distribution network. Each microgrid has its own renewable generation unit (ReGU) producing $P_{gi}(t)$, $i \in \mathcal{I}$, units of power at time t , which is stochastic in nature and is modeled by Geometric Brownian Motion (GBM) given by:

$$dP_{gi}(t) = \mu_{gi}P_{gi}(t)dt + \sigma_{gi}P_{gi}(t)dW_{ti}, \quad (1)$$

with an initial condition, $P_{gi}(0) > 0$, for all $i \in \mathcal{I}$. The constants μ_{gi} and σ_{gi} are the drift and volatility terms respectively and W_{ti} denotes a Wiener process. We empirically verify this

model assumption with RES generation data in Section V. The Weiner processes W_{ti}, W_{tj} are correlated according to

$$dW_{ti}dW_{tj} = \rho_{ij}dt, \quad i, j \in \mathcal{I}, \quad (2)$$

where ρ_{ij} is the correlation coefficient indicative of correlation between RES output of closely sited microgrids. Therefore,

$$dP_{gi}dP_{gj} = \sigma_i\sigma_j\rho_{ij}P_{gi}P_{gj}dt, \quad i, j \in \mathcal{I}. \quad (3)$$

Each microgrid also postulates a constant critical power demand of D_{ci} units, $i \in \mathcal{I}$, at a future time denoted as T_f . In IMMIG, the objective of the system is to satisfy power demand and supply balance at T_f , *almost surely* with minimum amount of resources collectively. In case of $P_{gi}(T_f) \geq D_{ci}$ for microgrid i , it can ensure sustained operation of its own load demand. In addition, the excess generation of $D_{ci} - P_{gi}(T_f)$ units can be used to supply the load demands of other microgrids, thus requiring less overall energy storage capacity to maintain grid reliability. Note, that this excess generation will need to be curtailed in IDMMG. On the other hand when $P_{gi}(T_f) < D_{ci}$, to avoid the risk of microgrid i not being able to meet the power demand of its critical loads, it can be supported by either excess renewable generation from other microgrids or the energy storage maintained by the DNO. To avail these benefits of IMMIG, microgrids participate in a contract with the DNO, which controls the energy transactions and battery allocation for the whole system by *independently* maintaining a portfolio consisting of fractions of ReGUs from each participant microgrid and centralized battery units. In particular, as shown in Fig. 1, the ReGUs in the portfolio of the DNO are physically located at the premises of the individual microgrid, thus following same dynamics (1), while the battery storage, being shared by all the microgrids, is fully controlled and allocated by the DNO. Considering the battery storage has the ability to dispatch in smaller units, each producing constant P_b units of power, the total available power in the portfolio maintained by the DNO at any time t is given by,

$$V(P_{g1}(t), \dots, P_{gN_m}(t), t) = \sum_{i=1}^{N_m} [a_i(t)P_{gi}(t)] + b(t)P_b, \quad (4)$$

where, $a_i(t), i \in \mathcal{I}$, is the number of ReGUs allocated from microgrid i and $b(t)$ is the number of battery units in the portfolio. At time $t = T_f$, we assume that a total of m , with $0 \leq m \leq N_m$, microgrids will have enough individual generation to supply their local demand. We denote the set of indices of the microgrids with sufficient generation at time T_f as \mathcal{I}_s , with $|\mathcal{I}_s| = m$, and let \mathcal{I}_d be the set of indices of the microgrids not capable of supplying their own local demand by renewable generation individually at time T_f ; thus $|\mathcal{I}_d| = N_m - m$. We have $P_{gi}(T_f) \geq D_{ci}$ if $i \in \mathcal{I}_s$ and $P_{gi}(T_f) < D_{ci}$ if $i \in \mathcal{I}_d$. The DNO is responsible for supporting the j^{th} microgrid, $j \in \mathcal{I}_d$, by utilizing either the surplus power (if available) from other microgrids, or the battery units in its portfolio. We remark that, the knowledge of the sets \mathcal{I}_s and \mathcal{I}_d are unknown *a priori* at initial time. Therefore, a focus on the time evolution of the ReGUs and the battery units from $t = 0$ till the time $t = T_f$ is required to guarantee that the demand is met at the requested time T_f . At time $t = T_f$, there are two possibilities:

(1) $\sum_{i=1}^{N_m} P_{gi}(T_f) \geq \sum_{i=1}^{N_m} D_{ci}$: In this case, collectively the microgrids have sufficient renewable generation to supply

critical load demands of each individual microgrid. Hence, no additional power from battery units is required.

(2) $\sum_{i=1}^{N_m} P_{gi}(T_f) < \sum_{i=1}^{N_m} D_{ci}$: Here, the total deficit of $\sum_{i=1}^{N_m} [D_{ci} - P_{gi}(T_f)]$ units of power is required to be maintained in the portfolio of the DNO to support the critical load demand of microgrid $j \in \mathcal{I}_d$, from the combination of battery units and surplus power, if any, from microgrid $i, i \in \mathcal{I}_s$. Note that, if microgrid $j \in \mathcal{I}_d$ also has a local battery storage, capable of supplying b_j kW of power, it can adjust its local demand from D_{cj} kW to $(D_{cj} - b_j)$ kW, which would be requested from the DNO, if required.

To address both the possibilities with minimum number of energy resources, the DNO needs to balance its own power portfolio (4). In this context, we introduce a constraint of *rated power conservation* of the portfolio, which requires:

$$\sum_{i=1}^{N_m} [da_i(t)P_{gi}(t)] + db(t)P_b = 0, \quad (5)$$

for $t \in (0, T_f)$ to ensure that the change in total power output of the generation portfolio due to the changes in the number of battery units and the number of ReGUs is zero; thus the change in total power generated by the portfolio maintained by DNO is only due to the change of renewable generation of individual microgrid. Thus, after initial allocation $a_i(0), i \in \mathcal{I}$, and $b(0)$, the DNO, at a future time t , can change the number of battery units but has to ensure that the power change is compensated by exchanging with the ReGUs in the portfolio. Therefore, the problem from the perspective of the DNO is:

Determine the number, $b(t)$ of battery blocks and number, $a_i(t)$ of renewable generation units based on $P_{gi}(t), i \in \mathcal{I}$,

$$\text{such that } \sum_{i=1}^{N_m} [da_i(t)P_{gi}(t)] + db(t)P_b = 0, \quad (6)$$

$$\sum_{i=1}^{N_m} [a_i(T_f)P_{gi}(T_f)] + b(T_f)P_b = \sum_{i=1}^{N_m} r_i [D_{ci} - P_{gi}(T_f)], \quad (7)$$

for $t \in (0, T_f)$, where $r_i = 1$ if $i \in \mathcal{I}_d$ and $r_i = 0$ if $i \in \mathcal{I}_s$.

Note that, under the *rated power conservation* constraint, finding the amount of initial battery units and initial ReGUs is essential for the DNO as having a lesser number of batteries and ReGUs has a risk of not being able to provide D_{ci} units of power at time T_f for all $i \in \mathcal{I}_d$, whereas provisioning more may result in excess energy produced at $t = T_f$ that will lead to a loss of revenue to the DNO. Section IV of this article presents the proposed strategy to find the resource allocation policy in real-time under both IDMMG and IMMIG framework. Our proposed strategy can be utilized to support critical infrastructures by providing guaranteed supply of critical demand even in islanded mode of operation.

IV. SOLUTION METHODOLOGY

A. Individualized Multi-microgrid System

First, we consider the case of IDMMG where power sharing among the microgrids is not possible and each microgrid is treated independently by the DNO *i.e.* available power in the portfolio maintained by the DNO for each microgrid is:

$$\hat{V}_i(P_{gi}(t), t) = \hat{a}_i(t)P_{gi}(t) + \hat{b}_i(t)P_b, \quad i \in \mathcal{I}, \quad (8)$$

and $0 \leq t \leq T_f$, where $\hat{a}_i(t)$, $\hat{b}_i(t)$ are the number of ReGUs and battery units allocated for microgrid i . In case of IDMMG, the *rated power conservation* constraint is given by:

$$d\hat{a}_i(t)P_{gi}(t) + d\hat{b}_i(t)P_b = 0, \text{ for all } i \in \mathcal{I}, \quad (9)$$

and the total amount of battery units maintained by DNO is:

$$\hat{b}(t) = \sum_{i=1}^{N_m} \hat{b}_i(t), \quad \forall t \in [0, T_f].$$

To ensure the power demand of i^{th} microgrid is met at the requested time T_f , the DNO needs to supply the deficit of $D_{ci} - P_{gi}(T_f)$ units of power from the portfolio if the microgrid is not capable of supplying its own demand from the renewable generation, and 0 otherwise. Therefore the power portfolio has to satisfy the following terminal condition,

$$\hat{V}_i(P_{gi}(T_f), T_f) = \begin{cases} 0 & \text{if } P_{gi}(T_f) \geq D_{ci} \\ D_{ci} - P_{gi}(T_f) & \text{if } P_{gi}(T_f) < D_{ci}. \end{cases} \quad (10)$$

As the amount of renewable generation at T_f is not deducible and also not known a priori due to inherent uncertainty [28], we provide a policy of maintaining the number of battery units, $\hat{b}_i(t)$ and ReGUs, $\hat{a}_i(t)$ for $t \in [0, T_f]$, satisfying the terminal condition (10), such that the critical demand of D_{ci} , $i \in \mathcal{I}$, units is met *almost-surely* at time T_f in the following theorem.

Theorem 1. *Under the rated power conservation constraint (9), suppose $\hat{a}_i(t)$ and $\hat{b}_i(t)$ are given by:*

$$\hat{a}_i(t) = -\Phi \left[\frac{\ln \left(\frac{D_{ci}}{P_{gi}(t)} \right) - \frac{\sigma_{gi}^2}{2} (T_f - t)}{\sigma_{gi} \sqrt{(T_f - t)}} \right],$$

$$\hat{b}_i(t) = \frac{D_{ci}}{P_b} \Phi \left[\frac{\ln \left(\frac{D_{ci}}{P_{gi}(t)} \right) + \frac{\sigma_{gi}^2}{2} (T_f - t)}{\sigma_{gi} \sqrt{(T_f - t)}} \right], \quad t \in [0, T_f]$$

where, $\Phi(\cdot)$ is the standard normal cumulative distribution function, then the terminal condition specified by (10) is satisfied almost surely at time T_f .

Proof. Please see Appendix B. \square

It follows that, in case of IDMMG, the total amount of battery units required by the DNO for all $t \in [0, T_f]$ is:

$$\hat{b}(t) = \sum_{i=1}^{N_m} \frac{D_{ci}}{P_b} \Phi \left[\frac{\ln \left(\frac{D_{ci}}{P_{gi}(t)} \right) + \frac{\sigma_{gi}^2}{2} (T_f - t)}{\sigma_{gi} \sqrt{(T_f - t)}} \right], \quad (11)$$

while the total power portfolio value at $t = T_f$ is:

$$\hat{V}(P_{g1}(T_f), \dots, P_{gN_m}(T_f), T_f) = \sum_{i=1}^{N_m} \max(D_{ci} - P_{gi}(T_f), 0).$$

B. Interconnected Multi-microgrid System

Let us now consider the case of IMMIG where the power available in the portfolio maintained by the DNO is given by (4). In contrast to the IDMMG, here a single power portfolio is maintained instead of N_m independent portfolios. The IMMIG needs to ensure that the DNO is able to make up for the deficit $D_{ci} - P_{gi}(T_f)$, $i \in \mathcal{I}_d$ at $t = T_f$ from the surplus generation $P_{gj}(T_f) - D_{cj}$, $j \in \mathcal{I}_s$, thus requiring less amount of centralized battery units $b(t)$. In the following sections, we

provide a policy of maintaining the number of shared battery units, $b(t)$ and ReGUs, $a_i(t)$, $i \in \mathcal{I}$ for all $t \leq T_f$, that ensures that the power deficit is optimally met with guarantees given the knowledge of \mathcal{I}_d and \mathcal{I}_s is unknown a priori. Let the value of power portfolio, V at any time $t \in [0, T_f]$ be denoted by V_t . In case of IMMIG, the terminal condition is given by,

$$V_{T_f} = \max \left(\sum_{i=1}^{N_m} (D_{ci} - P_{gi}(T_f)), 0 \right). \quad (12)$$

Finding an analytical solution to $a_i(t)$, $b(t)$ for all $t \in [0, T_f]$ under the terminal condition (12) is intractable due to higher dimensionality of (4) (see Appendix C). We provide a numerical solution in the following sections.

Let, $\eta_{gi} := \frac{\mu_{gi}}{\sigma_{gi}}$ and consider a function $\gamma_i(x) := e^{-\eta_{gi}x - \frac{1}{2}\eta_{gi}^2 t}$, and let the distribution function of Wiener process be denoted by, $F_{W_{ti}}(x) = \frac{1}{\sqrt{2\pi t}} \int_{-\infty}^x e^{-\frac{u^2}{2t}} du$, for all $i \in \mathcal{I}$. Then define,

$$F_{\hat{W}_{ti}}(x) := \int_{-\infty}^x \gamma_i(u) dF_{W_{ti}}(u) = \frac{1}{\sqrt{2\pi t}} \int_{-\infty}^x e^{-\frac{(u+\eta_{gi}t)^2}{2t}} du. \quad (13)$$

$F_{\hat{W}_{ti}}(x)$ is the distribution function of the stochastic process $\hat{W}_{ti} := W_{ti} + \eta_{gi}t$, where $\hat{W}_{ti} \sim \mathcal{N}(0, t)$ for all $i \in \mathcal{I}$. $\gamma_i(x)$ can be used to define a transformed probability measure given by (13). Let us denote the expected value of a random variable under this transformed probability measure by $\hat{\mathbb{E}}[\cdot]$. The following theorem provides the solution of V_t for all $t \in [0, T_f]$ under this transformed probability measure.

Theorem 2. *Given the rated power conservation constraint (5) for all $t \in [0, T_f]$, the solution of V_t under the transformed probability measure (13) is,*

$$V_t = \hat{\mathbb{E}}[\max(\sum_{i=1}^{N_m} (D_{ci} - P_{gi}(T_f)), 0)]. \quad (14)$$

Proof. Please see Appendix D. \square

Under the transformed probability measure, the value of V_t for any $t \leq T_f$ is the expected value of the portfolio at T_f , which can be calculated numerically [29], as described below, to find the provisioning policy of the ReGUs and battery units, $a_i(t)$, $i \in \mathcal{I}$ and $b(t)$ respectively, for $t \in [0, T_f]$.

Let the time horizon $[0, T_f]$ be partitioned into N equal intervals $0 = t_0 < t_1 < \dots < t_N = T_f$ such that $t_n = n\Delta t$, $n \in \{0, 1, \dots, N\}$ where $\Delta t = T_f/N$ denotes the length of each interval. The vector of renewable generation values at $t = t_n$ is denoted by $\mathbf{P}_{\mathcal{G}}(t_n) = [P_{g1}(t_n) \dots P_{gN_m}(t_n)]^T$. We assume that at the end of each time interval, each ReGU output can either increase or decrease by a constant factor of $u_i (\geq 1)$, $d_i (< 1)$ respectively, with respect to the current values, with certain probabilities. Here, $\mathbf{P}_{\mathcal{G}}(t_{n+1})$ can take one of the 2^{N_m} possible values with corresponding probabilities $P_k \in \mathbf{P} \in \mathbb{R}^{2^{N_m} \times 1}$ and $\sum_{k=1}^{2^{N_m}} P_k = 1$. The time evolution of $\mathbf{P}_{\mathcal{G}}(t_n)$ is shown in Fig. 2 for two consecutive time intervals and $N_m = 2$ for brevity of exposition. Without loss of generality, imposing the constraint, $u_i d_i = 1$, $i \in \mathcal{I}$, we can estimate the values of P_k , u_i , d_i , given $\mathbf{P}_{\mathcal{G}}(t_n)$, μ_{gi} , σ_{gi} , ρ_{ij} , $i, j \in \mathcal{I}$, by comparing the expectation, variance and covariance of the stochastic processes, under the transformed probability measure, with that from the discrete N_m -ary tree. The detailed procedure is given in Appendix A. Let $\mathbf{U} \in \mathbb{R}^{2^{N_m} \times N_m}$ denote a matrix

where k^{th} row of U contains the movement factors of $P_G(t_n)$ associated with probability $P_k, k \in \{1, 2, \dots, 2^{N_m}\}$. Once the values of P_k, u_i, d_i are determined, we divide the algorithm in three sequentially executed parts as explained below.

1) *Forward propagation*: Let us consider that our objective is to find the values of $a_i(t_n), i \in \mathcal{I}$ and $b(t_n)$ where $t_n < t_N = T_f$. Given the current value of the renewable generation vector, $P_G(t_n)$, first we estimate all possible values of $P_G(t_N)$ with corresponding probabilities as shown in Fig. 2. The general algorithm is given in Algorithm 2.

2) *Backward propagation*: Using the results obtained in the forward propagation step and values of $D_{ci}, i \in \mathcal{I}$, the value of V_{t_N} can be computed using (12) for all possible points at $t = t_N$. To estimate V_{t_n} , the portfolio value is back propagated from $t = t_N$ till t_n , using (14) at each $t_k, k \in \{N-1, N-2, \dots, n\}$. For example, in case of $N_m = 2$, as shown in Fig. 2, $V_{t_n} = \sum_{i=1}^4 P_i V_{t_{n+1}, i}$, where $V_{t_{n+1}, i}$ are estimated from preceding back propagation steps. The backpropagation algorithm is given in Algorithm 3.

3) *Resources calculation*: Once V_{t_n} is obtained, we can compute the values of $a_i(t_n)$ and $b(t_n)$ calculating the change in portfolio and renewable generation values obtained from forward and backward propagation as shown in Algorithm 1.

The entire algorithm is summarized in Algorithm 1. Each node in the implementation of tree data structure, shown in Fig. 2, has elements P_G , to contain ReGU output associated with the node, V , to store portfolio value of the node, p , which contains probability of encountering the node starting from initial time t_n , ohp , containing one hop probability of running into the node from its parent and an unique ID, id , assigned to each node. In the next section, we provide the simulation results of the algorithm where a IMM with two microgrids and a DNO, operating in hour-ahead market, is considered.

Algorithm 1: Dynamic Resource Allocation

Input : $P_G(t_n) = \{P_{gi}(t_n)\}_{i=1}^{N_m}, D_c = \{D_{ci}\}_{i=1}^{N_m},$
 $\mathbf{a} = \{a_i(t_{n-1})\}_{i=1}^{N_m}, P_b, T_f, N, \mathbf{P}, \mathbf{U};$
Output: $\mathbf{r} = \{r_i\}_{i=1}^{N_m+1}$ // Resource values
 /* Initialization */
 $\Delta t \leftarrow T_f/N; n \leftarrow t_n/\Delta t; \mathbf{L}, \mathbf{L}_n \leftarrow [];$
 $\mathbf{v} \leftarrow \vec{0} \in \mathbb{R}^{(2^{N_m}) \times 1}; \mathbf{r} \leftarrow \vec{0} \in \mathbb{R}^{(N_m+1) \times 1};$
 $\mathbf{A} \leftarrow \vec{0} \in \mathbb{R}^{2^{N_m} \times (N_m+1)}; \mathbf{A}[:, N_m+1] \leftarrow P_b;$
 /* Forward Propagation */
 $\mathbf{L} \leftarrow \text{FP}(N-n, \mathbf{U}, \mathbf{P}, P_G(t_n));$
 /* Backpropagation */
 $V_{t_n}, \mathbf{L}_n \leftarrow \text{BP}(\mathbf{L}, D_c);$
 /* Resources Calculation */
if $|\mathbf{L}_n| \neq 1$ **then**
 for $j = 1$ **to** 2^{N_m} **do**
 $c \leftarrow \mathbf{L}_n[j]; \mathbf{v}[j] \leftarrow V$ value of $c;$
 $\mathbf{p}_g \leftarrow P_G$ value of $c; \mathbf{A}[j, 1 : N_m] \leftarrow \mathbf{p}_g^T;$
 end
 $\mathbf{r} \leftarrow \mathbf{A}^\dagger \mathbf{b};$
else
 $\mathbf{r}[1 : N_m] \leftarrow \mathbf{a};$
 $\mathbf{r}[N_m+1] \leftarrow V_{t_n} - \mathbf{r}[1 : N_m]^T P_G(t_n);$
end
return $\mathbf{r};$

Algorithm 2: Forward Propagation

Function $\text{FP}(nStep, \mathbf{U}, \mathbf{P}, P_{GI})$:
 create *root* node with $id = 0, p = 1, P_G = P_{GI};$
 $\mathbf{L}_f \leftarrow [\text{root}]; pid \leftarrow 0;$
for $i = 1$ **to** $nStep$ **do**
 for $j = 1$ **to** $(2^{N_m})^i$ **do**
 $parent \leftarrow$ get node with $id = pid;$
 $pr \leftarrow p$ value of $parent$ node;
 $C_G \leftarrow P_G$ value of $parent$ node;
 for $k = 1$ **to** N_m **do**
 $child \leftarrow$ create new node;
 $child.P_G \leftarrow C_G \otimes U[k, :];$
 $child.p \leftarrow pr \otimes P[k];$
 $child.id \leftarrow (2^{N_m} \times pid) + k;$
 $child.ohp \leftarrow P[k];$
 append $child$ to $parent;$
 if $i = nStep$ **then**
 append $child$ to $\mathbf{L}_f;$
 end
 end
 $pid \leftarrow pid + 1;$
 end
end
return $\mathbf{L}_f;$

Algorithm 3: Backpropagation

Function $\text{BP}(\mathbf{L}, D_c)$:
foreach $c \in \mathbf{L}$ **do**
 $\mathbf{p}_g \leftarrow$ member P_G of node $c;$
 $tv \leftarrow \max(\sum_{i=1}^{N_m} [D_c - \mathbf{p}_g][i], 0);$
 update value of member V of c with $tv;$
end
 $\mathbf{L}_c, \mathbf{L}_n \leftarrow \mathbf{L}; end \leftarrow |\mathbf{L}_c|; ev \leftarrow tv;$
while $end \neq 1$ **do**
 $\mathbf{L}_p \leftarrow []; numNodes \leftarrow end;$
 while $numNodes > 0$ **do**
 $s \leftarrow 2^{N_m}$ siblings from $\mathbf{L}_c;$
 $\mathbf{v} \leftarrow V$ values of each node in $s;$
 $\mathbf{p}_s \leftarrow ohp$ values of each node in $s;$
 $parent \leftarrow$ parent node of siblings in $s;$
 $parent.V \leftarrow \sum_{i=1}^{2^{N_m}} \mathbf{v}[i] \mathbf{p}_s[i];$
 append $parent$ to $\mathbf{L}_p;$
 $numNodes \leftarrow numNode - 2^{N_m};$
 end
 $\mathbf{L}_c \leftarrow \mathbf{L}_p; end \leftarrow |\mathbf{L}_c|;$
 if $end = 2^{N_m}$ **then**
 $\mathbf{L}_n \leftarrow \mathbf{L}_c;$
 end
end
return $ev, \mathbf{L}_n;$

V. SIMULATION RESULTS

A. Model assumption verification

First we analyse the empirical wind power time series data to validate the model assumption (1) and estimate the parameters of the stochastic process. Wind generation data from the northwestern part of USA is taken from [30] for the

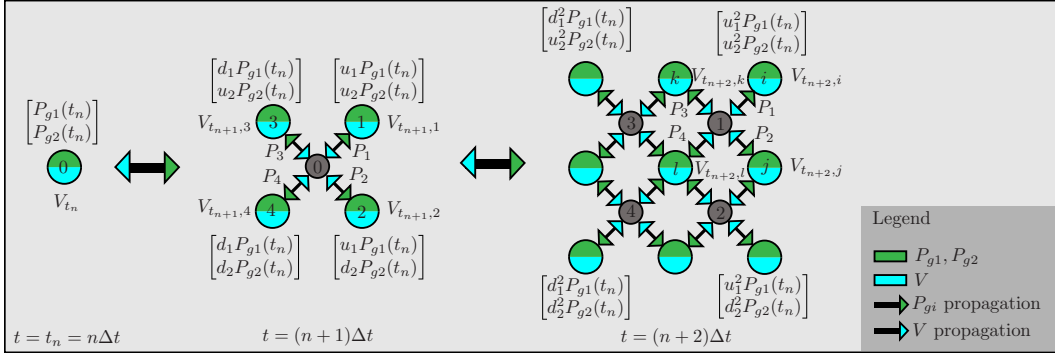


Fig. 2. Forward and backward propagation steps to calculate V_{t_n} for an IMMIG with 2 interconnected microgrids

month of June, 2020 at an interval of 5 minutes. As typical wind generation dynamics vary over different hours of a day [31], it is necessary to modify the parameters of (1) according to period of interest during a day. In our case, wind data from 10 a.m.-5 p.m. is chosen and maximum likelihood estimator is used to find drift and volatility parameters. The estimated drift and volatility parameters are 0.007 and 0.027 respectively with chi-square goodness of fit score of 18.86 including 13 degrees of freedom. The p -value, calculated from the goodness of fit test with significance level $\alpha = 0.05$, is 0.128 which justifies the validity of GBM model of wind power dynamics [32].

B. Parameters and sample size determination

For the simulation, two MGs with renewable generations, $P_{g1}(t)$ and $P_{g2}(t)$ with parameters $\mu_{g1} = 0.006$, $\sigma_{g1} = 0.03$ and $\mu_{g2} = 0.005$, $\sigma_{g2} = 0.04$ respectively, are considered and realized using discrete approximation of (1). We also assume that the generations are correlated with a correlation coefficient of $\rho_{12} = 0.6$ [31]. We assume that the battery unit power is $P_b = 1$ kW. The critical load demands, $D_{c1} = 20$ kW and $D_{c2} = 25$ kW, of the two MGs respectively, are to be met at $T_f = 5$ hrs. We use Algorithm 1 to compute optimal provisioning of initial resources and resource updates at each time instant, under rated power conservation constraint, that satisfies power balance at T_f . We assume that the ReGUs and the battery units are adjusted at an interval of one hour.

We first focus on the number of samples needed to arrive at meaningful statistical inferences. Fig. 3 shows the density histogram plot of $P_{g1}(t)$ for different time instants for two sample sets each containing 10000 samples of $P_{g1}(t)$ drawn from numerical simulation of the dynamic equation (1) with $\mu_{g1} = 0.006$, $\sigma_{g1} = 0.03$ and initial condition, $P_{g1}(0) = 20$ kW. Both sample sets consist of samples of $P_{g1}(t)$ with the terminal case of $P_{g1}(T_f) > D_{c1}$. We compare the distribution of the samples, at $t = 1, 2, \dots, 5$, in the two sample sets, using Two-sample Kolmogorov–Smirnov (KS) test [33] which produces KS statistics values 0.008, 0.01, 0.0062, 0.0079 and 0.0094 respectively. For sample size of 10000 in each set, the critical value of KS statistics is 0.019. The lower values of KS statistics than the critical value indicates that simulation of our algorithm for 10000 independent runs can produce highly stable results. Similar conclusions can be drawn for other terminal cases of $P_{g1}(T_f)$ and $P_{g2}(t)$, such as, $P_{g1}(T_f) \leq D_{c1}$, $P_{g2}(T_f) > D_{c2}$ and $P_{g2}(T_f) \leq D_{c2}$.

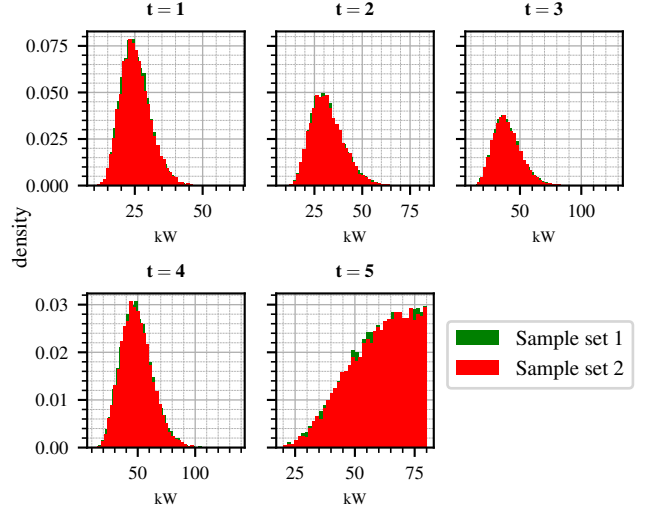
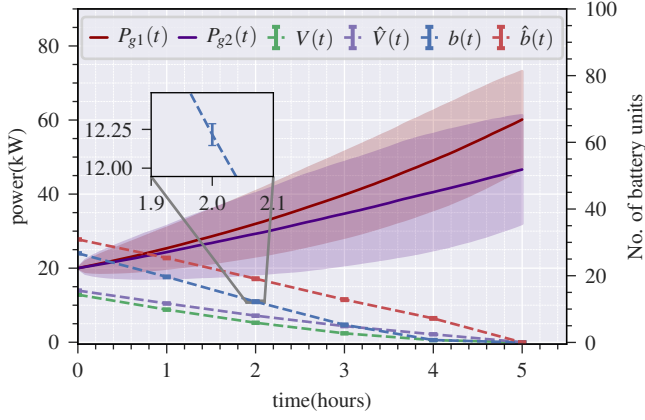


Fig. 3. Histograms of $P_{g1}(t)$ for $t \in \{1, 2, \dots, 5\}$ with two sample sets each containing 10000 samples of $P_{g1}(t)$ with terminal condition $P_{g1}(T_f) > D_{c1}$.

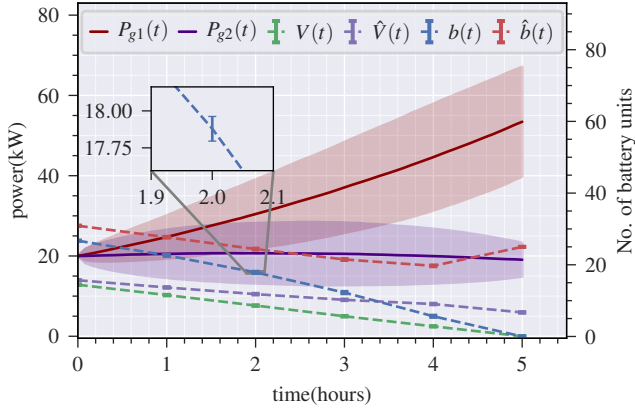
Here, in figures, Fig. 4, simulation results are shown for three sets of 10000 runs, each set satisfying different terminal conditions of $P_{g1}(T_f)$ and $P_{g2}(T_f)$ w.r.t D_{c1} and D_{c2} respectively, with mean values plotted for renewable generations along with standard deviations in shaded regions. For all other resources, mean values along with 95% bootstrap confidence interval (CI) around the mean, with 10000 bootstrap samples, are plotted. The narrow 95% CI around the means for battery requirement, power portfolio and BESS reduction, as seen from Fig. 4, indicate high confidence of the outcomes of our proposed algorithm. Implementation is done in Python 3.8.

C. Case study 1: $P_{g1}(T_f) \geq D_{c1}$, $P_{g2}(T_f) \geq D_{c1}$

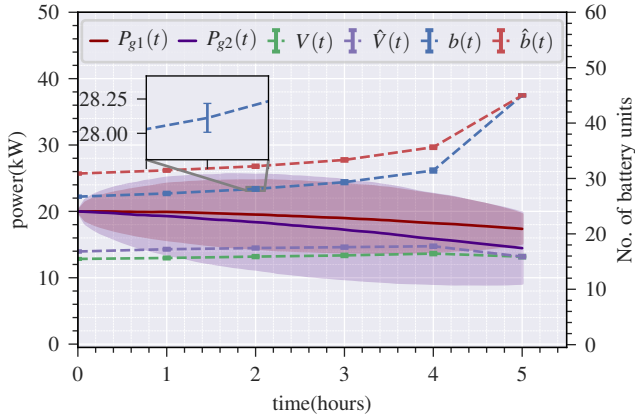
Fig. 4a illustrates the scenario where the renewable generations of both the MGs are sufficient to meet respective load demands at $t = T_f$. We remark that the algorithm has no knowledge of the terminal state *a priori* at any time $t < T_f$. We observe that the battery units requirement and the power portfolio value become 0 at $t = T_f$ as expected for both IDMMG and IMMIG. The trajectories of $b(t)$, $\hat{b}(t)$ and average reduction in battery units in IMMIG (shown in Table I and Fig. 5) reveal that IMMIG enables DNO to reduce battery



(a) Case study 1: $P_{g1}(T_f) \geq D_{c1}, P_{g2}(T_f) \geq D_{c2}$



(b) Case study 2: $P_{g1}(T_f) \geq D_{c1}, P_{g2}(T_f) < D_{c2}$



(c) Case study 3: $P_{g1}(T_f) < D_{c1}, P_{g2}(T_f) < D_{c2}$

Fig. 4. (a) Both MGs are capable of supplying their own demand at T_f , requiring no battery and power to be maintained in portfolio for both IDMMG ($\hat{V}(t), \hat{b}(t)$) and IMMIG ($V(t), b(t)$). (b) Excess generation from MG 1 is utilized to supply demand of MG 2 in IMMIG at T_f , whereas in IDMMG, average battery units' requirement is 25 to guarantee that the demand is met. (c) Both MGs are not capable of supplying own demand requiring same battery amount for both IDMMG and IMMIG. For all cases, power required in the portfolio is lower in IMMIG than IDMMG. Standard deviation of 10,000 realizations of $P_{g1}(t)$ and $P_{g2}(t)$ are shown in shaded regions with mean values plotted with solid lines. Zoomed inset, showing an example of 95% CI around the mean of battery requirement for IMMIG at $t=2$ hrs, indicates high confidence in average battery requirement of our proposed scheme.

requirement by 36.94% and the average reduction in initial battery requirement is 13.5% over IDMMG.

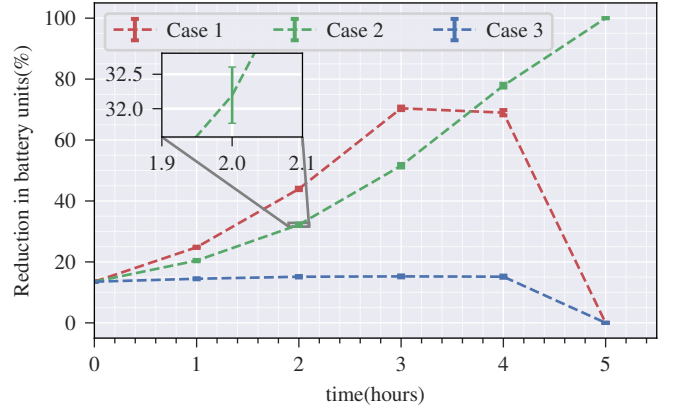


Fig. 5. Reduction in battery storage in IMMIG as a percentage of the same in IDMMG for three case studies. For all $t < T_f$, in IMMIG, DNO requires less amount of battery units compared to IDMMG while ensuring the demand is met at T_f for all cases. The narrow 95% CI around the mean battery reduction percentage, shown in zoomed inset at $t=2$ hrs for case 2 as example, indicates high confidence in average battery reduction in our proposed algorithm.

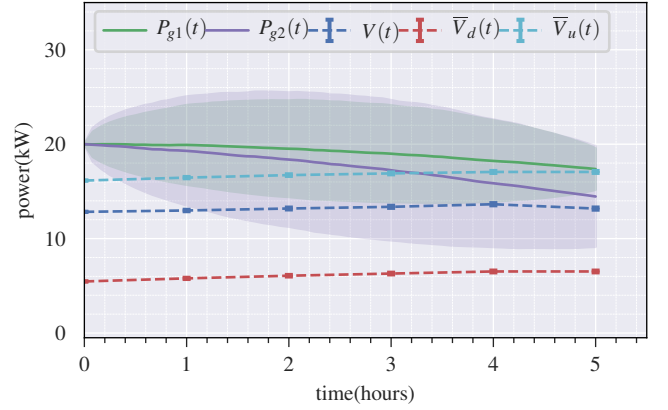


Fig. 6. Incorrect initial battery allocation leads to the risk of overproduction or underproduction. $\bar{V}_u(t)$ denotes the power portfolio trajectory when initial battery allocation is 20% more than optimal, $b(0)$, derived in Case 3. Here, at the end of the horizon, DNO has overproduction. $\bar{V}_d(t)$ shows the scenario when initial battery allocation is 20% less than optimal. Here, DNO cannot produce required power to support the critical loads at the requested time T_f .

TABLE I

Average BESS reduction (%) in IMMIG for three cases shown in Fig. 4a-4c.

| Time (hrs.) | $P_{g1}(T_f) \geq D_{c1}$ | $P_{g1}(T_f) \geq D_{c1}$ | $P_{g1}(T_f) < D_{c1}$ |
|-------------|---------------------------|---------------------------|------------------------|
| | $P_{g2}(T_f) \geq D_{c2}$ | $P_{g2}(T_f) < D_{c2}$ | $P_{g2}(T_f) < D_{c2}$ |
| 0 | 13.50 | 13.50 | 13.50 |
| 1 | 24.80 | 20.43 | 14.66 |
| 2 | 43.96 | 32.19 | 15.20 |
| 3 | 70.41 | 51.57 | 15.49 |
| 4 | 68.98 | 77.85 | 15.31 |
| 5 | 0 | 100 | 0 |
| Overall | 36.94 | 49.26 | 12.36 |

D. Case study 2: $P_{g1}(T_f) \geq D_{c1}, P_{g2}(T_f) < D_{c1}$

Fig. 4b illustrates the scenario where microgrid 1 is capable of supplying its load demand of $D_{c1} = 20$ kW but renewable generation of microgrid 2 is not sufficient to meet $D_{c2} = 25$ kW at $t = T_f$ (here too the terminal state is not available *a priori* at any time $t < T_f$). Here the power deficit of

microgrid 2 is more than the surplus generated from microgrid 1. The plot shows that at the end of the time horizon, IMMIG enables DNO to utilize the surplus thus requiring no battery unit at $t = T_f$ whereas in case of IDMMG, average battery units' requirement is 25 to guarantee that the demand is met. Moreover, average reduction in battery units, for the entire time horizon, is 49.26%, as shown in Table I and Fig. 5. The value of the power portfolio, as shown in Fig. 4b, becomes 0 at T_f in case of IMMIG while IDMMG requires DNO to have the power deficit of microgrid 2 in its power portfolio.

E. Case study 3: $P_{g1}(T_f) < D_{c1}, P_{g2}(T_f) < D_{c2}$

Fig. 4c captures the scenario where both the microgrids are not capable of meeting their load demands at $t = T_f$. In this case the power portfolio value required by the DNO is equal to the net deficit of the microgrids for both IDMMG and IMMIG settings. The battery units requirement is nearly equal to the net load demand of the whole system while in case of IMMIG, the average reduction over IDMMG, on initial battery units requirement and overall battery requirement are 13.50% and 12.25% respectively, as shown in Table I and Fig. 5.

Next we demonstrate the optimality of the initial amount of battery reserve allocation derived by our proposed algorithm. Fig. 6 illustrates the scenario, under case 3 in IMMIG, when initial battery allocation by the DNO is not optimal as derived in Section IV-B. In Fig. 6, $\bar{V}_u(t)$ denotes the power portfolio trajectory when initial battery allocation is 20% more than optimal and $V(t)$ denotes the optimal power portfolio. We can see that, at the end of the horizon, DNO has overproduction. $\bar{V}_d(t)$ denotes the scenario when initial battery allocation is 20% less than optimal. In this case, DNO cannot provide the critical loads at the end of the horizon, as the power in the portfolio is not sufficient to support the combined production deficit of the MGs. Similar plots can be shown for case 1 and 2 also, which are omitted to conserve space. Thus our algorithm enables DNO to provide assurance of meeting the demand of the MGs, without overproduction or underproduction, which enhances the system reliability.

The results corroborate the efficacy and utility of our resource allocation strategy in IMMIG with respect to BESS requirements while providing provable guarantees of meeting the power needs at the end of the prescribed horizons, which is an indispensable requirement for critical facilities. Therefore, it can be concluded that our proposed algorithm enables DNO to mitigate the uncertainty of supplying the demand of the microgrids at the requested time while reducing the battery requirement, thus enhancing grid reliability and efficiency.

VI. CONCLUSION

This article develops a novel energy management strategy for an IMMIG containing multiple microgrids, equipped with DER and critical infrastructure loads, and a DNO with centralized battery storage, with the focus of efficient energy storage allocation in real-time, to meet the load demands of the microgrids at the requested time with *almost sure guarantee*. Explicit stochastic model of wind generation is considered to represent the uncertainties of renewable generations. The proposed algorithms mitigate the uncertainties of meeting the load demands of the microgrids, due to intermittent renewable

generations, at the requested time, with *almost sure* guarantee which is an absolute requirement for critical infrastructures under catastrophic events. We also derive the energy storage allocation policy for IDMMG with no energy sharing facilities and compare the results with IMMIG. The simulation study shows that IMMIG enables DNO to have lower amount of battery storage than IDMMG, while still maintaining the guarantee of meeting the load demands of each microgrid.

APPENDIX A

PROBABILITIES AND CHANGE FACTORS CALCULATION

Applying Ito's lemma [34] to $d(\log P_{gi}(t))$,

$$\begin{aligned} d(\log P_{gi}(t)) &= \frac{\partial(\log P_{gi}(t))}{\partial P_{gi}(t)} dP_{gi}(t) + \frac{\partial^2(\log P_{gi}(t))}{\partial P_{gi}^2(t)} \frac{(dP_{gi}(t))^2}{2} \\ &= -\frac{\sigma_{gi}^2}{2} dt + \sigma_{gi} d\hat{W}_{ti} = -\frac{\sigma_{gi}^2}{2} dt + \sigma_{gi} \sqrt{dt} Z, \end{aligned}$$

where, $Z \sim \mathcal{N}(0, 1)$ and $dP_{gi}(t) = \sigma_{gi} P_{gi}(t) d\hat{W}_{ti}$. Let $X_n^i = \log P_{gi}(t_n)$. Therefore,

$$\hat{\mathbb{E}}[X_{n+1}^i - X_n^i] = -\frac{\sigma_{gi}^2}{2} \Delta t, \quad \text{Var}(X_{n+1}^i - X_n^i) = \sigma_{gi}^2 \Delta t.$$

Under the transformed probability measure (13), from (2),

$$\text{Corr}((X_{n+1}^i - X_n^i), (X_{n+1}^j - X_n^j)) = \rho_{ij} \sigma_{gi} \sigma_{gj} \Delta t.$$

Let \mathcal{I}_i denote the set of indices of probabilities associated with upward movement of $P_{gi}(t_n)$ and $\mathcal{I}_{ij} = (\mathcal{I}_i \cap \mathcal{I}_j) \cup (\mathcal{I}_i^c \cap \mathcal{I}_j^c)$, for all $i, j \in \mathcal{I}$. Let $h_i = \log u_i, i \in \mathcal{I}$, then,

$$-\frac{\sigma_{gi}^2}{2} \Delta t = h_i (\sum_{k \in \mathcal{I}_i} P_k - \sum_{k \notin \mathcal{I}_i} P_k), \quad (15a)$$

$$\sigma_{gi}^2 \Delta t = h_i^2 (\sum_{k=1}^{2^{N_m}} P_k) - h_i^2 (\sum_{k \in \mathcal{I}_i} P_k - \sum_{k \notin \mathcal{I}_i} P_k)^2, \quad (15b)$$

$$\rho_{ij} \sigma_{gi} \sigma_{gj} \Delta t = h_i h_j (\sum_{k \in \mathcal{I}_{ij}} P_k - \sum_{k \notin \mathcal{I}_{ij}} P_k), \quad (15c)$$

$$1 = \sum_{k=1}^{2^{N_m}} P_k. \quad (15d)$$

The above set of equations can be solved to find the values of $P_k, k \in \{1, 2, \dots, 2^{N_m}\}, u_i, d_i, i \in \mathcal{I}$.

APPENDIX B

PROOF OF THEOREM 1

The dynamics of $P_{gi}(t)$ is governed by (1). Since P_b is constant, $dP_b = 0$. In the subsequent development, explicit dependency of variables on t is omitted for brevity of notation. Applying differentiation operator to \hat{V}_i , given in (8), we have,

$$d\hat{V}_i = \hat{a}_i dP_{gi} + \hat{d}_i P_{gi} + \hat{b}_i dP_b + \hat{d}_b P_b. \quad (16)$$

Under the constraint (9) for $t \in [0, T_f]$ and $i \in \mathcal{I}$, (16) becomes

$$d\hat{V}_i = \hat{a}_i dP_{gi} + \hat{b}_i dP_b = \hat{a}_i (\mu_{gi} P_{gi} dt + \sigma_{gi} P_{gi} dW_{ti}), \quad (17)$$

Applying Ito's lemma [34] and considering infinitesimal dt ,

$$\begin{aligned} d\hat{V}_i &= \frac{\partial \hat{V}_i}{\partial t} dt + \frac{\partial \hat{V}_i}{\partial P_{gi}} dP_{gi} + \frac{1}{2} \frac{\partial^2 \hat{V}_i}{\partial P_{gi}^2} (dP_{gi}^2) \\ &= \frac{\partial \hat{V}_i}{\partial t} dt + \frac{\partial \hat{V}_i}{\partial P_{gi}} (\mu_{gi} dt + \sigma_{gi} dW_{ti}) P_{gi} + \frac{\sigma_{gi}^2 P_{gi}^2}{2} \frac{\partial^2 \hat{V}_i}{\partial P_{gi}^2} dt. \quad (18) \end{aligned}$$

Using, (17) and (18) we get,

$$\begin{aligned} &\left[\frac{\partial \hat{V}_i}{\partial t} + \mu_{gi} P_{gi} \frac{\partial \hat{V}_i}{\partial P_{gi}} + \frac{1}{2} \sigma_{gi}^2 P_{gi}^2 \frac{\partial^2 \hat{V}_i}{\partial P_{gi}^2} - \hat{a}_i \mu_{gi} P_{gi} \right] dt \\ &+ \left[\sigma_{gi} P_{gi} \frac{\partial \hat{V}_i}{\partial P_{gi}} - \hat{a}_i \sigma_{gi} P_{gi} \right] dW_{ti} = 0. \quad (19) \end{aligned}$$

Note that, if $\hat{a}_i = \frac{\partial \hat{V}_i}{\partial P_{gi}}$ then $[\sigma_{gi} P_{gi} \frac{\partial \hat{V}_i}{\partial P_{gi}} - \hat{a}_i \sigma_{gi} P_{gi}] = 0$, which eliminates the uncertainty. Thus,

$$\frac{\partial \hat{V}_i}{\partial t} + \frac{1}{2} \sigma_{gi}^2 P_{gi}^2 \frac{\partial^2 \hat{V}_i}{\partial P_{gi}^2} = 0. \quad (20)$$

Now, to ensure that the critical demand is met *almost surely* at the requested time T_f , we need to solve (20) with the terminal condition (10) and find $\hat{a}_i(t)$, $\hat{b}_i(t)$.

Let $\tau = T_f - t$, $x_i = \ln(P_{gi})$ for all $i \in \mathcal{I}$. Therefore, $\frac{\partial \hat{V}_i}{\partial t} = -\frac{\partial \hat{V}_i}{\partial \tau}$, $\frac{\partial \hat{V}_i}{\partial P_{gi}} = \frac{1}{P_{gi}} \frac{\partial \hat{V}_i}{\partial x_i}$, $\frac{\partial^2 \hat{V}_i}{\partial P_{gi}^2} = \frac{1}{P_{gi}^2} \left[\frac{\partial^2 \hat{V}_i}{\partial x_i^2} - \frac{\partial \hat{V}_i}{\partial x_i} \right]$. From (20),

$$\frac{\partial \hat{V}_i}{\partial \tau} = \frac{1}{2} \sigma_{gi}^2 \frac{\partial^2 \hat{V}_i}{\partial x_i^2} - \frac{1}{2} \sigma_{gi}^2 \frac{\partial \hat{V}_i}{\partial x_i} = A_i \frac{\partial^2 \hat{V}_i}{\partial x_i^2} + B_i \frac{\partial \hat{V}_i}{\partial x_i}, \quad (21)$$

where, $A_i = \frac{1}{2} \sigma_{gi}^2$ ($A_i > 0$), $B_i = -\frac{1}{2} \sigma_{gi}^2$. From (10), the final condition on power portfolio $\hat{V}_i(P_{gi}(t), t = T_f)$, or equivalently, initial condition on $\hat{V}_i(x_i, \tau = 0)$ is given as:

$$\hat{V}_i(x_i, 0) = \begin{cases} 0 & \text{if } x_i \geq \ln(D_{ci}) \\ D_{ci} - e^{x_i} & \text{if } x_i < \ln(D_{ci}). \end{cases} \quad (22)$$

Let $\hat{V}_i(x_i, \tau) = e^{-(\alpha_i x_i + \beta_i \tau)} \hat{u}_i(x_i, \tau)$, where $\alpha_i, \beta_i \in \mathbb{R}$. Then, $\frac{\partial \hat{V}_i}{\partial \tau} = e^{-(\alpha_i x_i + \beta_i \tau)} (\frac{\partial \hat{u}_i}{\partial \tau} - \beta_i \hat{u}_i)$, $\frac{\partial \hat{V}_i}{\partial x_i} = e^{-(\alpha_i x_i + \beta_i \tau)} (\frac{\partial \hat{u}_i}{\partial x_i} - \alpha_i \hat{u}_i)$, $\frac{\partial^2 \hat{V}_i}{\partial x_i^2} = e^{-(\alpha_i x_i + \beta_i \tau)} (\frac{\partial^2 \hat{u}_i}{\partial x_i^2} - 2\alpha_i \frac{\partial \hat{u}_i}{\partial x_i} + \alpha_i^2 \hat{u}_i)$.

Therefore, using (21),

$$\frac{\partial \hat{u}_i}{\partial \tau} - \beta_i \hat{u}_i = A_i \left[\frac{\partial^2 \hat{u}_i}{\partial x_i^2} - 2\alpha_i \frac{\partial \hat{u}_i}{\partial x_i} + \alpha_i^2 \hat{u}_i \right] + B_i \left[\frac{\partial \hat{u}_i}{\partial x_i} - \alpha_i \hat{u}_i \right],$$

and thus,

$$\frac{\partial \hat{u}_i}{\partial \tau} = A_i \frac{\partial^2 \hat{u}_i}{\partial x_i^2} + [B_i - 2\alpha_i A_i] \frac{\partial \hat{u}_i}{\partial x_i} + [\beta_i + \alpha_i^2 A_i - \alpha_i B_i] \hat{u}_i.$$

Choosing $\alpha_i = \frac{B_i}{2A_i}$, $\beta_i = \frac{B_i^2}{4A_i}$, we get, $\frac{\partial \hat{u}_i}{\partial \tau} = A_i \frac{\partial^2 \hat{u}_i}{\partial x_i^2}$. Solution of this partial differential equation [35] is given

by $\hat{u}_i(x_i, \tau) = \frac{1}{\sqrt{4\pi A_i \tau}} \int_{-\infty}^{\infty} \hat{u}_i(y, 0) e^{-\frac{(x_i - y)^2}{4A_i \tau}} dy$. Since, $\hat{V}_i(y, 0) = e^{-(\alpha_i y)} \hat{u}_i(y, 0)$, and $\alpha_i = \frac{B_i}{2A_i}$, $\beta_i = \frac{B_i^2}{4A_i}$,

$$\begin{aligned} \hat{u}_i(x_i, \tau) &= \frac{1}{\sqrt{4\pi A_i \tau}} \int_{-\infty}^{\infty} e^{-\frac{(x_i - y)^2}{4A_i \tau}} e^{\alpha_i y} \hat{V}_i(y, 0) dy \\ &= \frac{1}{\sqrt{4\pi A_i \tau}} \int_{-\infty}^{\infty} e^{-\left[\frac{(y - B_i \tau - x_i)^2}{4A_i \tau} - \frac{B_i x_i}{2A_i} - \frac{B_i^2 \tau}{4A_i} \right]} \hat{V}_i(y, 0) dy \\ &= \frac{1}{\sqrt{4\pi A_i \tau}} \int_{-\infty}^{\infty} e^{-\left[\frac{(y - B_i \tau - x_i)^2}{4A_i \tau} \right]} e^{(\alpha_i x_i + \beta_i \tau)} \hat{V}_i(y, 0) dy. \end{aligned} \quad (23)$$

Therefore, $\hat{V}_i(x_i, \tau)$ is given by $e^{-(\alpha_i x_i + \beta_i \tau)} \hat{u}_i(x_i, \tau)$, which can be further expanded as:

$$\begin{aligned} &\frac{1}{\sqrt{4\pi A_i \tau}} \int_{-\infty}^{\infty} e^{-\left[\frac{(y - B_i \tau - x_i)^2}{2\sqrt{A_i \tau}} \right]^2} \hat{V}_i(y, 0) dy \\ &= \frac{1}{\sigma_{gi} \sqrt{2\pi \tau}} \int_{-\infty}^{\infty} e^{-\frac{1}{2} \left[\frac{(y + \frac{\sigma_{gi}^2}{2} \tau - x_i)}{\sigma_{gi} \sqrt{\tau}} \right]^2} \hat{V}_i(y, 0) dy. \end{aligned} \quad (24)$$

Applying the initial condition (22) to $\hat{V}_i(y, 0)$ we get:

$$\begin{aligned} \hat{V}_i(x_i, \tau) &= \frac{1}{\sigma_{gi} \sqrt{2\pi \tau}} \left[\int_{-\infty}^{\ln(D_{ci})} e^{-\frac{1}{2} \left[\frac{(y + \frac{\sigma_{gi}^2}{2} \tau - x_i)}{\sigma_{gi} \sqrt{\tau}} \right]^2} (D_{ci} - e^y) dy \right] \\ &= \underbrace{\frac{D_{ci}}{\sigma_{gi} \sqrt{2\pi \tau}} \left[\int_{-\infty}^{\ln(D_{ci})} e^{-\frac{1}{2} \left[\frac{(y + \frac{\sigma_{gi}^2}{2} \tau - x_i)}{\sigma_{gi} \sqrt{\tau}} \right]^2} dy \right]}_{I_1} \end{aligned}$$

$$- \underbrace{\frac{1}{\sigma_{gi} \sqrt{2\pi \tau}} \left[\int_{-\infty}^{\ln(D_{ci})} e^{-\frac{1}{2} \left[\frac{(y + \frac{\sigma_{gi}^2}{2} \tau - x_i)}{\sigma_{gi} \sqrt{\tau}} \right]^2} e^y dy \right]}_{I_2}.$$

Let, $z_i = \frac{1}{\sigma_{gi} \sqrt{\tau}} (y + (\frac{\sigma_{gi}^2}{2})\tau - x_i) \implies dz_i = \frac{1}{\sigma_{gi} \sqrt{\tau}} dy$. Then,

$$I_1 = \frac{D_{ci}}{\sqrt{2\pi}} \int_{-\infty}^{\frac{\ln(D_{ci}) + \frac{\sigma_{gi}^2}{2} \tau - x_i}{\sigma_{gi} \sqrt{\tau}}} e^{-\frac{z_i^2}{2}} dz_i = D_{ci} \Phi \left[\frac{\ln(D_{ci}) + \frac{\sigma_{gi}^2}{2} \tau}{\sigma_{gi} \sqrt{\tau}} \right],$$

where, $\Phi(\cdot)$ is the Cumulative Distribution Function (CDF) of the standard Gaussian random variable $\sim \mathcal{N}(0, 1)$. Similarly,

$$I_2 = \frac{e^x}{\sqrt{2\pi}} \int_{-\infty}^{\frac{\ln(D_{ci}) + \frac{\sigma_{gi}^2}{2} \tau - x_i}{\sigma_{gi} \sqrt{\tau}}} e^{-\frac{1}{2} [z_i - \sigma_{gi} \sqrt{\tau}]^2} dz_i. \quad (25)$$

Let, $w_i = z_i - \sigma_{gi} \sqrt{\tau}$, $\implies dw_i = dz_i$. Therefore, from (25),

$$I_2 = P_{gi} \Phi \left[\frac{\ln(D_{ci}) - \frac{\sigma_{gi}^2}{2} \tau}{\sigma_{gi} \sqrt{\tau}} \right],$$

where, $\Phi(\cdot)$ is the CDF of the standard Gaussian random variable $\sim \mathcal{N}(0, 1)$. Therefore, substituting the value of τ ,

$$\begin{aligned} \hat{V}_i(P_{gi}(t), t) &= (D_{ci}) \Phi \left[\frac{\ln\left(\frac{D_{ci}}{P_{gi}(t)}\right) + \frac{\sigma_{gi}^2}{2} (T_f - t)}{\sigma_{gi} \sqrt{(T_f - t)}} \right] \\ &\quad - P_{gi}(t) \Phi \left[\frac{\ln\left(\frac{D_{ci}}{P_{gi}(t)}\right) - \frac{\sigma_{gi}^2}{2} (T_f - t)}{\sigma_{gi} \sqrt{(T_f - t)}} \right]. \end{aligned} \quad (26)$$

Comparing equation (26) with equation (8),

$$\hat{a}_i(t) = -\Phi \left[\frac{\ln\left(\frac{D_{ci}}{P_{gi}(t)}\right) - \frac{\sigma_{gi}^2}{2} (T_f - t)}{\sigma_{gi} \sqrt{(T_f - t)}} \right], \quad (27)$$

$$\hat{b}_i(t) = \frac{D_{ci}}{P_b} \Phi \left[\frac{\ln\left(\frac{D_{ci}}{P_{gi}(t)}\right) + \frac{\sigma_{gi}^2}{2} (T_f - t)}{\sigma_{gi} \sqrt{(T_f - t)}} \right].$$

This completes the proof.

APPENDIX C

DERIVATION OF STOCHASTIC DIFFERENTIAL EQUATION OF V_t IN IMMIG FOR RES UNCERTAINTY MITIGATION

From (1) and for constant P_b (i.e. $dP_b = 0$), and under the *rated power conservation* (5), applying Ito's lemma [34] on differential of V_t and considering infinitesimal dt , we obtain:

$$\frac{\partial V_t}{\partial t} dt + \sum_{i=1}^{N_m} \frac{\partial V_t}{\partial P_{gi}} dP_{gi} + \sum_{i=1}^{N_m} \sum_{j=1}^{N_m} \frac{\partial^2 V_t}{2 \partial P_{gi} \partial P_{gj}} dP_{gi} dP_{gj} = \sum_{i=1}^{N_m} a_i dP_{gi}.$$

Using (1) and (3),

$$\begin{aligned} &\left[\frac{\partial V_t}{\partial t} + \sum_{i=1}^{N_m} \mu_{gi} P_{gi} \frac{\partial V_t}{\partial P_{gi}} + \frac{1}{2} \sum_{i=1}^{N_m} \sum_{j=1}^{N_m} \sigma_{gi} \sigma_{gj} \rho_{ij} \frac{\partial^2 V_t}{\partial P_{gi} \partial P_{gj}} P_{gi} P_{gj} \right. \\ &\quad \left. - \sum_{i=1}^{N_m} a_i \mu_{gi} P_{gi} \right] dt = \sum_{i=1}^{N_m} \left[a_i \sigma_{gi} P_{gi} - \frac{\partial V_t}{\partial P_{gi}} \sigma_{gi} P_{gi} \right] dW_{ti}. \end{aligned}$$

Note that, if $a_i = \frac{\partial V_t}{\partial P_{gi}}$, for all $i \in \mathcal{I}$, uncertainty associated with all the renewable generation is eliminated, and we have:

$$\frac{\partial V_t}{\partial t} + \frac{1}{2} \sum_{i=1}^{N_m} \sum_{j=1}^{N_m} \sigma_{gi} \sigma_{gj} \rho_{ij} P_{gi} P_{gj} \frac{\partial^2 V_t}{\partial P_{gi} \partial P_{gj}} = 0. \quad (28)$$

Note that, if there are numerous MGs present in the IMMIG ($N_m \gg 1$), theoretical solution of (28) to find $a_i(t)$, $b(t)$, under the terminal condition (12), becomes intractable.

APPENDIX D
PROOF OF THEOREM 2

Given the dynamics of RES (1), we can find the value of V_t , $t \in [0, T_f]$, given the terminal condition (12), by changing the probability measure using (13). From (1), for all $i \in \mathcal{I}$,

$$\begin{aligned} dP_{gi}(t) &= \mu_{gi}P_{gi}(t)dt + \sigma_{gi}P_{gi}(t)(d\hat{W}_{ti} - \eta_{gi}dt) \\ &= \sigma_{gi}P_{gi}(t)d\hat{W}_{ti}. \end{aligned} \quad (29)$$

Applying differentiation operator to (4) and since P_b is constant, $dV_t = \sum_{i=1}^{N_m} a_i dP_{gi} = \sum_{i=1}^{N_m} a_i \sigma_{gi} P_{gi} d\hat{W}_{ti}$. Therefore, for any $t \in [0, T_f]$, $V_{T_f} = V_t + \int_t^{T_f} \sum_{i=1}^{N_m} a_i \sigma_{gi} P_{gi} d\hat{W}_{ti}$. Hence, under the transformed probability measure, the expected value of V_{T_f} , calculated at t , where $t \in [0, T_f]$ is,

$$\begin{aligned} \hat{\mathbb{E}}[V_{T_f}] &= V_t + \hat{\mathbb{E}}\left[\int_t^{T_f} \sum_{i=1}^{N_m} a_i \sigma_{gi} P_{gi} d\hat{W}_{ti}\right] \\ &= V_t + \int_t^{T_f} \sum_{i=1}^{N_m} a_i \sigma_{gi} P_{gi} \hat{\mathbb{E}}[d\hat{W}_{ti}] = V_t, \end{aligned}$$

where, the last equality follows from the fact that $\hat{\mathbb{E}}[d\hat{W}_{ti}] = 0$, under the transformed probability measure (13). From (12),

$$V_t = \hat{\mathbb{E}}\left[\max\left(\sum_{i=1}^{N_m} (D_{ci} - P_{gi}(T_f)), 0\right)\right].$$

This completes the proof.

REFERENCES

- [1] IRENA, "Global energy transformation: A roadmap to 2050," 2019, [Accessed 31 August 2020]. [Online]. Available: https://www.irena.org/-/media/Files/IRENA/Agency/Publication/2019/Apr/IRENA_Global_Energy_Transformation_2019.pdf
- [2] Y. Yang, S. Bremner, C. Menictas, and M. Kay, "Battery energy storage system size determination in renewable energy systems: A review," *Renewable and Sustainable Energy Reviews*, vol. 91, pp. 109–125, 2018.
- [3] H. Zou, S. Mao, Y. Wang, F. Zhang, X. Chen, and L. Cheng, "A survey of energy management in interconnected multi-microgrids," *IEEE Access*, vol. 7, pp. 72 158–72 169, 2019.
- [4] L. Che, X. Zhang, M. Shahidehpour, A. Alabdulwahab, and A. Abusorrah, "Optimal interconnection planning of community microgrids with renewable energy sources," *IEEE Transactions on Smart Grid*, vol. 8, no. 3, pp. 1054–1063, 2015.
- [5] S. A. Arefifar, M. Ordóñez, and Y. A.-R. I. Mohamed, "Energy management in multi-microgrid systems—development and assessment," *IEEE Transactions on Power Systems*, vol. 32, no. 2, pp. 910–922, 2016.
- [6] S. Salinas, M. Li, P. Li, and Y. Fu, "Dynamic energy management for the smart grid with distributed energy resources," *IEEE Transactions on Smart Grid*, vol. 4, no. 4, pp. 2139–2151, 2013.
- [7] J. Wu and X. Guan, "Coordinated multi-microgrids optimal control algorithm for smart distribution management system," *IEEE Transactions on Smart Grid*, vol. 4, no. 4, pp. 2174–2181, 2013.
- [8] Y. Liu, H. B. Gooi, Y. Li, H. Xin, and J. Ye, "A secure distributed transactive energy management scheme for multiple interconnected microgrids considering misbehaviors," *IEEE Transactions on Smart Grid*, vol. 10, no. 6, pp. 5975–5986, 2019.
- [9] T. Li and M. Dong, "Residential energy storage management with bidirectional energy control," *IEEE Transactions on Smart Grid*, vol. 10, no. 4, pp. 3596–3611, 2018.
- [10] B. Zhao, X. Wang, D. Lin, M. M. Calvin, J. C. Morgan, R. Qin, and C. Wang, "Energy management of multiple microgrids based on a system of systems architecture," *IEEE Transactions on Power Systems*, vol. 33, no. 6, pp. 6410–6421, 2018.
- [11] Y. Xu, H. Sun, and W. Gu, "A novel discounted min-consensus algorithm for optimal electrical power trading in grid-connected dc microgrids," *IEEE Transactions on Industrial Electronics*, vol. 66, no. 11, pp. 8474–8484, 2019.
- [12] W. Liu, W. Gu, J. Wang, W. Yu, and X. Xi, "Game theoretic non-cooperative distributed coordination control for multi-microgrids," *IEEE Transactions on Smart Grid*, vol. 9, no. 6, pp. 6986–6997, 2018.
- [13] S. Park, J. Lee, S. Bae, G. Hwang, and J. K. Choi, "Contribution-based energy-trading mechanism in microgrids for future smart grid: A game theoretic approach," *IEEE Transactions on Industrial Electronics*, vol. 63, no. 7, pp. 4255–4265, 2016.
- [14] H. Alharbi and K. Bhattacharya, "Stochastic optimal planning of battery energy storage systems for isolated microgrids," *IEEE Transactions on Sustainable Energy*, vol. 9, no. 1, pp. 211–227, 2017.
- [15] H. Farzin, M. Fotuhi-Firuzabad, and M. Moeini-Aghtaie, "Enhancing power system resilience through hierarchical outage management in multi-microgrids," *IEEE Transactions on Smart Grid*, vol. 7, no. 6, pp. 2869–2879, 2016.
- [16] H.-I. Su and A. El Gamal, "Modeling and analysis of the role of energy storage for renewable integration: Power balancing," *IEEE Transactions on Power Systems*, vol. 28, no. 4, pp. 4109–4117, 2013.
- [17] Y. Zhang, Z. Y. Dong, F. Luo, Y. Zheng, K. Meng, and K. P. Wong, "Optimal allocation of battery energy storage systems in distribution networks with high wind power penetration," *IET Renewable Power Generation*, vol. 10, no. 8, pp. 1105–1113, 2016.
- [18] A. Maleki, M. G. Khajeh, and M. Ameri, "Optimal sizing of a grid independent hybrid renewable energy system incorporating resource uncertainty, and load uncertainty," *International Journal of Electrical Power & Energy Systems*, vol. 83, pp. 514–524, 2016.
- [19] K. W. Hedman and G. B. Sheblé, "Comparing hedging methods for wind power: Using pumped storage hydro units vs. options purchasing," in *2006 International Conference on Probabilistic Methods Applied to Power Systems*. IEEE, 2006, pp. 1–6.
- [20] H. Verdejo, A. Awerkin, E. Saavedra, W. Kliemann, and L. Vargas, "Stochastic modeling to represent wind power generation and demand in electric power system based on real data," *Applied Energy*, vol. 173, pp. 283–295, 2016.
- [21] M. Olsson, M. Perninge, and L. Söder, "Modeling real-time balancing power demands in wind power systems using stochastic differential equations," *Electric Power Systems Research*, vol. 80, no. 8, pp. 966–974, 2010.
- [22] S. Cui, Y.-W. Wang, C. Li, and J.-W. Xiao, "Prosumer community: A risk aversion energy sharing model," *IEEE Transactions on Sustainable Energy*, vol. 11, no. 2, pp. 828–838, 2019.
- [23] X. Yang, H. He, Y. Zhang, Y. Chen, and G. Weng, "Interactive energy management for enhancing power balances in multi-microgrids," *IEEE Transactions on Smart Grid*, vol. 10, no. 6, pp. 6055–6069, 2019.
- [24] Y. Han, K. Zhang, H. Li, E. A. A. Coelho, and J. M. Guerrero, "Mas-based distributed coordinated control and optimization in microgrid and microgrid clusters: A comprehensive overview," *IEEE Transactions on Power Electronics*, vol. 33, no. 8, pp. 6488–6508, 2017.
- [25] S. Cui, Y.-W. Wang, Y. Shi, and J.-W. Xiao, "A new and fair peer-to-peer energy sharing framework for energy buildings," *IEEE Transactions on Smart Grid*, vol. 11, no. 5, pp. 3817–3826, 2020.
- [26] M. B. Shadmand and R. S. Balog, "Multi-objective optimization and design of photovoltaic-wind hybrid system for community smart dc microgrid," *IEEE Transactions on Smart Grid*, vol. 5, no. 5, pp. 2635–2643, 2014.
- [27] L. Olatomiwa, S. Mekhilef, M. S. Ismail, and M. Moghavvemi, "Energy management strategies in hybrid renewable energy systems: A review," *Renewable and Sustainable Energy Reviews*, vol. 62, pp. 821–835, 2016.
- [28] F. Black and M. Scholes, "The pricing of options and corporate liabilities," *Journal of political economy*, vol. 81, no. 3, pp. 637–654, 1973.
- [29] J. C. Cox, S. A. Ross, and M. Rubinstein, "Option pricing: A simplified approach," *Journal of financial Economics*, vol. 7, no. 3, pp. 229–263, 1979.
- [30] B. B. Authority, "Wind generation and total load in the bpa balancing authority," 2020, [Accessed 1 August 2020]. [Online]. Available: <https://transmission.bpa.gov/business/operations/wind/>
- [31] B. Ernst, Y.-H. Wan, and B. Kirby, "Short-term power fluctuation of wind turbines: Analyzing data from the german 250-mw measurement program from the ancillary services viewpoint," National Renewable Energy Lab., Golden, CO (US), Tech. Rep., 1999.
- [32] M. Natrella et al., "Nist/sematech e-handbook of statistical methods," *Nist/Sematech*, vol. 49, 2010.
- [33] M. Hollander, D. A. Wolfe, and E. Chicken, *Nonparametric statistical methods*. John Wiley & Sons, 2013, vol. 751.
- [34] C. Gardiner, *Stochastic methods*. Springer Berlin, 2009, vol. 4.
- [35] L. C. Evans, *Partial differential equations*. American Mathematical Soc., 2010, vol. 19.